A&A 427, 593–605 (2004)
DOI: 10.1051/0004-6361:20041224

Astronomy & Astrophysics

Interpretation of the variability of the β Cephei star λ Scorpii*

II. The line-profile diagnostics

K. Uytterhoeven[1,2], J. H. Telting[3], C. Aerts[1,4], and B. Willems[5,6]

[1] Institute of Astronomy, Catholic University Leuven, Celestijnenlaan 200 B, 3001 Leuven, Belgium
e-mail: katrien.uytterhoeven@ster.kuleuven.ac.be
[2] Mercator Telescope, Calle Alvarez de Abreu 70, 38700 Santa Cruz de La Palma, Spain
[3] Nordic Optical Telescope, Apartado 474, 38700 Santa Cruz de La Palma, Spain
[4] Department of Astrophysics, University of Nijmegen, PO Box 9010, 6500 GL Nijmegen, The Netherlands
[5] Department of Physics and Astronomy, Northwestern University, 2145 Sheridan Road, Evanston, IL 60208, USA
[6] Department of Physics and Astronomy, The Open University, Milton Keynes, MK7 6AA, UK

Received 4 May 2004 / Accepted 15 July 2004

Abstract. We present the results of our analysis of a time series of high-resolution spectra of the multiple β Cephei star λ Scorpii. The data set has a total time-span of more than 5000 days and includes an intensive monitoring campaign during 8 consecutive nights. We confirm the presence of a dominant frequency $f_1 = 4.679410$ c d^{-1} in the data. We show that the amplitude is variable in time according to the light-time effect in the multiple system. The dominant frequency is identified as a prograde dipole pulsation mode. From modelling of the amplitudes and phases across the profiles we derive pulsational parameters, the inclination angle $70° \leq i \leq 90°$ and $v \sin i \sim 125$ km s^{-1}. From a comparison between theoretically calculated forcing eigenfrequencies induced by the close companion and the eigenfrequencies of the observed oscillation mode we find no tidal enhancement or excitation of the pulsation mode of λ Scorpii. We find indications for the presence of additional frequencies with low amplitudes.

Key words. stars: binaries: spectroscopic – stars: oscillations – line: profiles – stars: individual: λ Scorpii

1. Introduction

With the goal to study the role of tidal effects on the excitation and/or enhancement of pulsation modes we have set up a project concerning the detailed analysis of the intrinsic variations of β Cephei stars in close binary systems. For the background of this observational program we refer to Uytterhoeven et al. (2004b, hereafter termed Paper I). In a rotating star, non-radial pulsations (NRP) reflect themselves as features moving from blue to red or vice versa through the line profile due to the Doppler effect (Vogt & Penrod 1983). High-resolution spectroscopy turned out to be a useful tool to study the line-profile variations (LPV) caused by NRP in full detail. Over the last years several quantitative methods for the extraction of information about the pulsation modes from the LPV have been developed, such as the Moment Method (Briquet & Aerts 2003 for the latest version) and the IPS (Intensity Period Search) Method (Telting & Schrijvers 1997). In the current work, we combine these different mode-identification techniques in order to model the pulsational behaviour of the multiple β Cephei star λ Scorpii.

The triple system λ Scorpii (HD 158926, HR 6527, 35 Sco, $\alpha_{2000} = 17^{\rm h}33^{\rm m}36\overset{\rm s}{.}52$, $\delta_{2000} = -37°06'13.8''$, $m_V = 1.62$, B1.5IV+B2V, 216 ± 42 pc) consists of a B1.5IV star in a $5\overset{\rm d}{.}9525$ eccentric ($e = 0.26$) orbit with most likely a T Tauri star and a B2V star that moves around the close orbit with a period of $1082^{\rm d}$ in an orbit with $e = 0.23$ (Paper I). The close pair is an eclipsing binary. In the current paper, we focus on the detailed analysis of line-profile variations of the primary of the system. This intrinsic variability has been studied already by Shobbrook & Lomb (1972) and Lomb & Shobbrook (1975) by means of photometric observations. They found a dominant period of $P_1 = 0\overset{\rm d}{.}2137015$ in combination with its first harmonic $P_2 = 0\overset{\rm d}{.}10685075$ and classified the star as a β Cephei star. The longer period $P_3 = 10\overset{\rm d}{.}1605$ in their dataset was attributed to the orbital movement. Watson (1988), treating the system as a single star, interpreted the variability with P_1 in terms of a radial oscillation. De Mey et al. (1997) already confirmed the dominant period by means of a line-profile study of a set of high-resolution spectra. They explained the variability in terms

* Based on observations obtained with the Coudé Echelle Spectrograph on the ESO CAT telescope and with the CORALIE Echelle Spectrograph on the 1.2-m Euler Swiss telescope, both situated at La Silla, Chile.

of NRP and found indications for the presence of more than one mode.

The fast rotation of the main component of λ Scorpii, together with its close binary nature, make this star a suitable object to study the relation between mode selection, mode amplitudes, tides and rotation, if any. The outline of this paper is as follows. In Sect. 2 we present the data. In Sect. 3 we report the results of the frequency analysis. Section 4 deals with the mode identification of the detected pulsation frequencies. In Sect. 5 we examine the possibility of a resonant excitation. The conclusions can be found in Sect. 6.

2. Data and grayscale representations

We refer to Paper I for a description of the data and data reduction, as well as a logbook of the observations. The complex character of the pulsation becomes visible in the grayscale representations of the 421 spectra obtained during 8 consecutive nights in July 1997 shown in Fig. 1. The individual plots show the residual Si III 4552.654 Å profiles of one night with respect to the average profile of the 421 spectra, displayed as a grayscale plot. Black denotes a positive flux and white indicates a negative flux with respect to the mean. The result is a complex pattern of black and white bands, which run into each other. Such a pattern, if interpreted in terms of oscillations, can only be the result from interactions between two or more NRP modes and cannot be reconciled with the suggestion of a radial mode by Watson (1988). The latter author, however, treated the object as a single star while we showed in Paper I that it is composed of a low-mass ($M_2 \sim 2\ M_\odot$) pre-main sequence star (to be ignored in the analysis of the Si III 4552.654 Å line) and two very similar early B stars. Through a detailed spectral analysis, the primary was found to have a temperature of 25 000 K, $\log g = 3.8$, $M \simeq 11\ M_\odot$ while the parameters of the third component are 22 000 K, $\log g = 4.0$, $M \simeq 9\ M_\odot$. Therefore we expect that the tertiary contributes significantly to the photometry and also to the profiles shown in Fig. 1. We cannot observe the third component directly in the profiles because the rotational broadening of the primary is larger than the velocity shifts of the orbit. This situation is analoguous to the one of the binary β Cephei star β Crucis, which is composed of a B0.5III primary and a B2V companion in a low-amplitude eccentric 5-yr orbit (Aerts et al. 1998). Given that the tertiary of λ Scorpii is also situated in the β Cephei instability strip (Pamyatnykh 1999), we cannot exclude it to be a pulsating star as well and to contribute to the complex patterns shown in Fig. 1. While the dominant frequency f_1, as already discussed in Paper I, is clearly due to the primary, any results of this work pointing to low-amplitude variability may either be due to the primary or the tertiary.

To remove the influence of the motion in the triple system we used the orbital parameters determined in Paper I, which we subsequently fed into the code KOREL (Hadrava 1995). We have tried to disentangle the observed profiles into contributions of the primary, secondary and tertiary component, but in doing so the KOREL code did not return realistic average profiles for the secondary and tertiary component. This is not too surprising as we are dealing with a complex triple

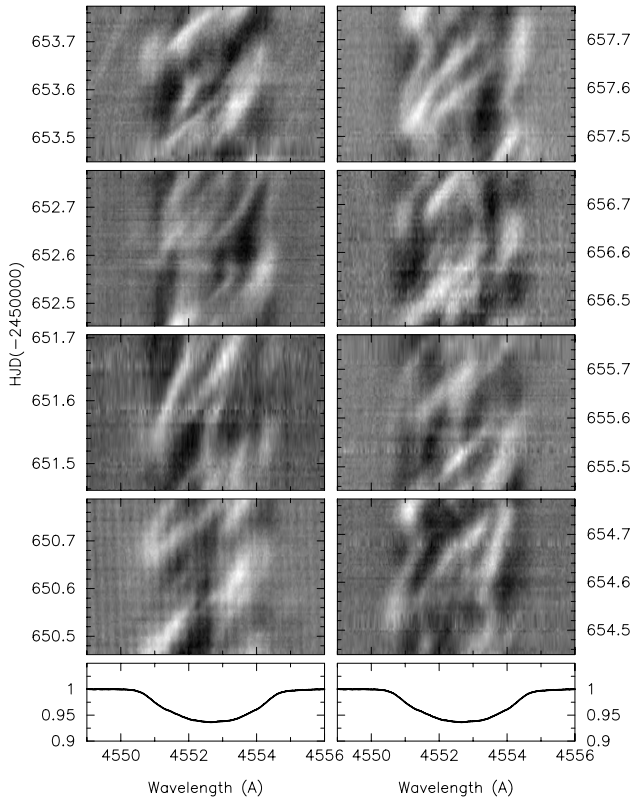

Fig. 1. Grayscale representations of the observed line profiles obtained during eight consecutive nights from 20–28 July 1997. The residual Si III 4552.654 Å profiles with respect to the average profile of the eight nights are plotted in a shade of gray: black represents a positive residual while white represents a negative residual. Bottom: the average profile of the eight nights.

system, the wide orbit of which is not very accurately determined. Therefore, we have only used KOREL to determine the average overal blended profile of the three components, together with the residual spectra calculated in the restframe of the primary. The orbit-corrected profiles are subsequently reconstructed by adding the O–C residuals to the average profile. This implies that the profiles still contain the blend with the line of the tertiary (the one of the secondary is negligible given that it is a much cooler star) as explained in the previous paragraph. We fed only the good-quality spectra of our dataset, i.e. those with a signal-to-noise ratio higher than 100 and those that didn't suffer from vignetting, into KOREL. In the next section we present the study of the intrinsic variations of λ Scorpii based on those 748 shifted Si III line profiles.

3. Frequency analysis

As mentioned in the introduction, only one pulsation frequency, together with its first harmonic, has been detected so far (Shobbrook & Lomb 1972; Lomb & Shobbrook 1975; De Mey et al. 1997). However, from the grayscale plots (see Fig. 1) we expect the presence of more than one intrinsic frequency.

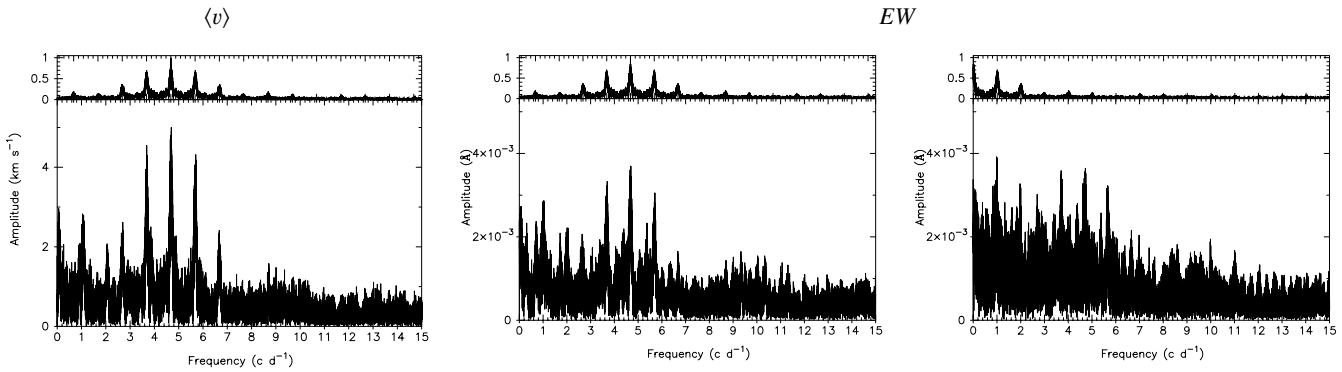

Fig. 2. Lomb-Scargle periodogram of the centroid radial velocity (*left*) and of the equivalent width (*middle and right*) derived from the profiles near 4552 Å (*left and middle*) and 4568 Å (*right*). On top of each figure the window function, shifted according to the highest peak in the periodogram, is given.

3.1. The variability of the dominant frequency

In Paper I, we have pointed out that the variability of the main frequency suggested by Lomb & Shobbrook (1975) from their photometric data is entirely compatible with the light-time effect in the multiple system. Here, we check if the different line diagnostics derived from our spectroscopic data allow us to find independent signatures of the variability of the main frequency.

We used different frequency analysis methods on the three first normalised moments ($\langle v \rangle$, $\langle v^2 \rangle$ and $\langle v^3 \rangle$) and on the equivalent width (*EW*) calculated from the Si III profiles at 4552.654 Å and 4567.872 Å of the 748 spectra after correction for the orbital motions. For a definition of the moments $\langle v^n \rangle$ of a line profile we refer to Aerts et al. (1992). A short description of the results of the analysis on the radial velocities (first normalised moment) of the shifted spectra was already given in Paper I.

The periodicity search was carried out by means of Phase Dispersion Minimisation (PDM, Stellingwerf 1978), the Lomb-Scargle method (Scargle 1982) and the CLEAN algorithm (Roberts et al. 1987), of which the latter two are based on Fourier techniques. For the PDM method we used the bin- and cover structures (5, 2) and (10, 3); for the CLEAN algorithm we used gain values 0.2 and 0.8. As the dataset of 748 spectra, covering a time-span of more than 5000 days, enables us to find frequencies up to an accuracy of 0.000005 c d^{-1} according to the empirically derived formula by Cuypers (1987), we searched for frequencies between 0 and 15 cycles per day (c d^{-1}), with frequency steps of 10^{-6} c d^{-1}. A conservative estimate of the error on the frequencies is given by the half width at half maximum amplitude of the highest peak of the window function, which turns out to be 0.00035 c d^{-1}.

In the variations of the *EW* of the profiles we find only evidence for the dominant pulsation frequency near 4.67942 c d^{-1} (Lomb & Shobbrook 1975). This frequency is more pronouncedly present in the Si III 4552.654 Å line than in the 4567.872 Å line due to a lower noise level of the former, as one can see on the Lomb-Scargle periodograms in Fig. 2. The variability of the *EW* has an amplitude of only 2% for the bluest Si III line.

From their photometric data, Lomb & Shobbrook (1975) found one dominant period of $0\overset{d}{.}2137015 \pm 0.0000006$ (this unrealistic small error is given by the authors) which corresponds to $f_{\rm phot} = 4.67942$ c d^{-1}. All analysis methods performed on the first three normalised velocity moments calculated from the two Si III lines resulted in a similar frequency. We end up with a dominant frequency in the first moment of the Si III 4552.654 Å (Si III 4567.872 Å) profile at 4.676672 c d^{-1} (4.676685 c d^{-1}). We estimate the intrinsic error on the frequencies to be 0.000013 c d^{-1}. This dominant frequency is related to the frequency $f_{\rm phot} = 4.67942$ c d^{-1}, by means of a one year alias. In the accuracy of our dataset we can rewrite $f_{\rm phot}$ as $f_1 = 4.679410$ c d^{-1}. We accept f_1 as the true main intrinsic frequency as the time spread of the photometric data is better suited to disentangle the alias patterns. The first harmonic of f_1, although clearly present in the photometric data of Lomb & Shobbrook (1975), is not found in the variability of $\langle v \rangle$ and $\langle v^3 \rangle$. Contrarily to that, $2f_1$ is present at low amplitude in the variations of $\langle v^2 \rangle$. This is what one would expect for a linear non-axisymmetric NRP mode (Aerts et al. 1992). Analyses of the moments of the bluest Si III profile led to similar results as those for the 4567.872 Å profile. Figure 2 shows the Lomb-Scargle periodogram of $\langle v \rangle$, calculated from the 4552.654 Å profile.

Figure 3 shows the phase diagrams of the first three normalised moments of the shifted Si III 4552.654 Å line. The fit to the second moment $\langle v^2 \rangle$ takes, besides the contribution of $f_1 = 4.679410$ c d^{-1}, also the contribution of $2f_1$ into account, while the fit to the third moment $\langle v^3 \rangle$ includes f_1, $2f_1$ and $3f_1$. The three fits reduce the variability with 45%, 36% and 42% in respectively $\langle v \rangle$, $\langle v^2 \rangle$ and $\langle v^3 \rangle$.

After prewhitening this dominant signal by subtracting synthetic sinusoidal curves with f_1 and its first harmonic $2f_1$, we continued the search for other candidate frequencies. As can been seen in Fig. 4, frequencies similar to f_1 (which is indicated by a dashed line), and its aliases, were still prominently present in the residuals, also after a CLEAN analysis with a high gain value and many iterations. Prewhitening with either $f_1 = 4.679410$ c d^{-1} or its alias 4.676672 c d^{-1} resulted in similar periodograms. In order to try and study the variability of f_1, as reported by Lomb & Shobbrook (1975) and explained in

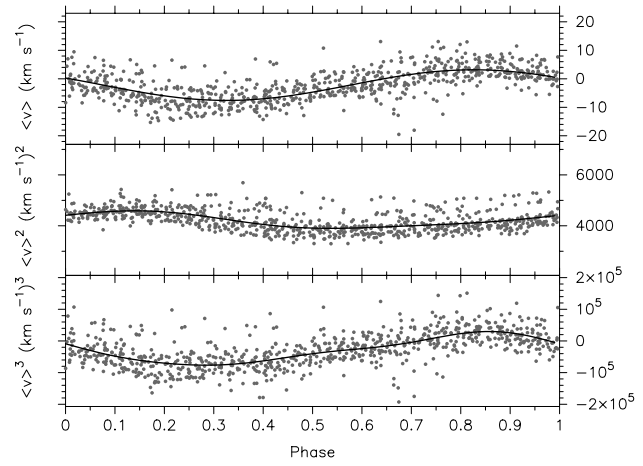

Fig. 3. The first three normalised moments of the Si III 4552.654 Å line of λ Scorpii folded with $f_1 = 4.679410$ c d^{-1}. The three fits take respectively f_1; f_1 and $2f_1$; f_1, $2f_1$ and $3f_1$ into account.

terms of the light-time effect in Paper I, further, we performed the following tests.

We divided the whole dataset, spanning 5000 days, in several subsets in order to investigate the change of amplitude of f_1 over the years. Unfortunately, due to the irregular time sampling of the data, we only have 2 subsets with a large amount of datapoints and a sufficient phase distribution for f_1, namely the subsets of 1995 and 1997 containing 3 respectively 8 nights of intensive monitoring. These subsets are too short to determine the change in f_1 due to the light-time effect from Fourier analysis or PDM. Moreover, the orbital velocity of those data is not very different so that the frequency change due to the light-time effect is very small for these epochs. Therefore, we checked first of all if amplitude variations occur. For the subsets of 1995 (June 1995), 1997 (all data) and a subset containing only the data of the 8 nights of 1997, we calculated the amplitude of f_1, respectively f_1 and $2f_1$, together with its error, for $\langle v \rangle$, respectively $\langle v^2 \rangle$. We did a similar test for the alias frequency 4.676672 c d^{-1}. The results are given in Table 1 and are illustrated in Fig. 5. We conclude that the amplitude of f_1 in $\langle v \rangle$ and $\langle v^2 \rangle$ for June 1995 differs significantly from the one of July 1997. The dataset of all data of 1997, spanning 1 year, shows signs of an averaging out of the amplitude. We cannot discriminate between the alias frequencies 4.679410 c d^{-1} and 4.676672 c d^{-1} as both frequencies fit the two first velocity moments equally well. The variable amplitude is either due to an unresolved beat pattern, or to the variability of the main frequency, or to both phenomena together. In the first case, one expects the effect of the frequency f_1 to disappear after prewhitening whenever it concerns a beat between two or more independent oscillation frequencies, which is not what we observe. We conclude that the variability of the amplitudes is most likely induced by the light-time effect.

Additionally we tried to find evidence for the change of value of the dominant frequency from non-linear fitting. In order to do so, we searched for the best-fitting value of f_1 in the first moment of the 4552.654 Å and 4567.872 Å profiles of the full dataset, the subset of June 1995 and the 8 nights of July 1997, by means of a non-linear least-squares fit, treating f_1 as a free parameter. In all cases the resulting value of f_1 depended very much on the given initial value and all obtained fits explained the variability equally well. Therefore we conclude that we cannot discriminate between 4.679410 c d^{-1} and 4.676672 c d^{-1} or any other peak very close to these frequencies in the subsets of the spectroscopic data.

From these tests, together with the observed phenomenon that signatures of f_1 still remain in the intrinsic variations after prewhitening and the fact that the remaining peaks ($f \in [4.671; 4.698]$ c d^{-1}) cannot be related to the prewhitened one by means of the window function, we conclude that λ Scorpii shows a variable frequency in its spectra but we are unable to quantify the change in the frequency due to the poor sampling.

3.2. Additional frequencies

The search for additional frequencies turned out to be very difficult. After prewhitening with f_1, a forest of peaks appeared at the interval 0–2.0 c d^{-1}, with no agreement in the candidate frequencies between $\langle v \rangle$, $\langle v^2 \rangle$ and $\langle v^3 \rangle$.

As we cannot remove the influence of the dominant frequency completely, the search for additional frequencies is very difficult because the convolution of the remaining peaks near f_1 with the window function implies a complex pattern in the periodograms. Nevertheless, candidate frequencies appear at low amplitudes. The second and third moment indicate the presence of a peak at 5.340978 c d^{-1} and the first and third moment show variability with a frequency at 3.899013 c d^{-1}. Both frequencies cannot be related to the dominant first frequency by means of the window function.

As an indicator for the significance of additional frequencies, one can use the 4 signal-to-noise criterion (4 *S/N*, Breger et al. 1993). This criterion is used to retain only frequencies with amplitudes higher than 4 times the noise level. The noise level is defined as the average amplitude of the remaining peaks in a restricted region of the periodogram after prewhitening with all candidate frequencies. In the case of the full dataset of λ Scorpii, the application of this criterion is by no means straightforward. Indeed, the remaining variability at frequencies near f_1 and the strong aliasing effect induce the presence of several additional peaks, as shown in Fig. 6 which lead to a high noise level at local positions in the periodogram. To determine the noise level, we selected the two "alias peak free" regions ([4.1;4.6] and [5.1;5.6] c d^{-1}) indicated by gray boxes in Fig. 6. For each box we calculated the average amplitude of the 50 highest remaining peaks, using frequency step 10^{-6} c d^{-1}, after prewhitening with f_1, $2f_1$ and the two candidate additional frequencies mentioned above. An average of these two values led to a noise level *S/N* of 0.91 (4 *S/N* = 3.64) km s^{-1} respectively 61.9 (4 *S/N* = 247) (km s^{-1})^2 for $\langle v \rangle$ and $\langle v^2 \rangle$. According to the 4 *S/N* criterion, applied to the full dataset, we have to reject the two candidate frequencies (see Table 3). We emphasize, however, that the definition of the noise level is ambiguous for λ Scorpii due to the remaining power at f_1 and its aliases.

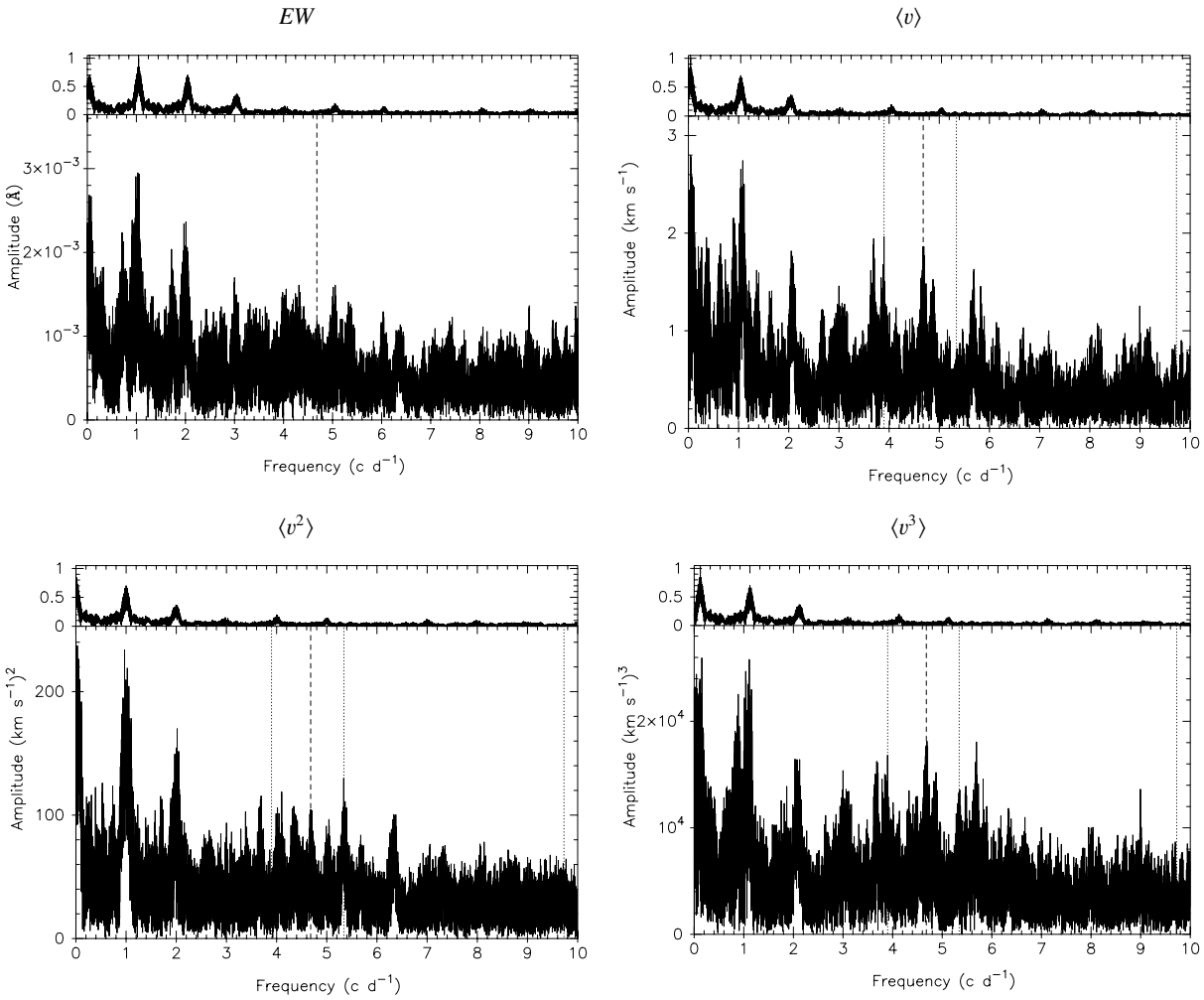

Fig. 4. Lomb-Scargle periodograms of the residuals of the equivalent width and of the first three velocity moments calculated from the 4552.654 Å profiles after prewhitening with frequency $f_1 = 4.679410$ c d^{-1} and its first harmonic. A frequency similar to f_1 (dashed line) is still present in the variability of the moments. Candidate additional frequencies $f_2 = 3.899013$ c d^{-1}, $f_3 = 5.340978$ c d^{-1} and $f_4 = 9.726644$ c d^{-1} are indicated by dotted lines. On top of each figure the window function, shifted according to the highest peak in the periodogram, is given.

Table 1. Overview of the range of amplitudes (amplitude plus/minus its standard error) of the contribution of 4.679410 c d^{-1} and 4.676672 c d^{-1} to the variability of $\langle v \rangle$, respectively $\langle v^2 \rangle$, obtained from a fit with f, respectively f and $2f$, calculated from the different subsets of data. The amplitudes are expressed in km s^{-1}, respectively (km s^{-1})^2. The total variance reduction is also given.

		4552.654 Å			4567.872 Å		
	Frequency	June 1995	1997	July 1997	June 1995	1997	July 1997
$\langle v \rangle$	4.679410 c d^{-1}	[5.32; 5.91]	[5.87; 6.29]	[6.03; 6.43]	[4.90; 5.47]	[6.17; 6.72]	[6.25; 6.78]
		71.17%	65.03%	68.30%	69.45%	56.81%	59.16%
	4.676672 c d^{-1}	[5.32; 5.91]	[5.67; 6.11]	[6.01; 6.43]	[4.90; 5.47]	[5.94; 6.51]	[6.17; 6.71]
		71.13%	61.08%	67.69%	69.60%	53.12%	57.53%
$\langle v^2 \rangle$	4.679410 c d^{-1}	[371; 405]	[362; 387]	[363; 387]	[411; 448]	[396; 425]	[385; 414]
		78.47%	71.19%	72.48%	79.61%	67.52%	67.54%
	4.676672 c d^{-1}	[372; 406]	[362; 387]	[362; 386]	[411; 448]	[390; 419]	[383; 411]
		78.81%	70.03%	72.05%	79.77%	65.47%	66.74%

3.3. Restriction to the intensive monitoring campaign

For the restricted dataset of 421 spectra, obtained on 8 consecutive nights in July 1997, prewhitening with the dominant frequency f_1 does not leave signatures in the variations of the residuals. We hence used this subset to check the presence of candidate frequencies. This subset leads to a much better defined noise level in the periodograms, but cannot lead to very precise frequency values. Indeed, this intensive subset covering 8 nights allows a frequency resolution of only 0.001 c d^{-1}.

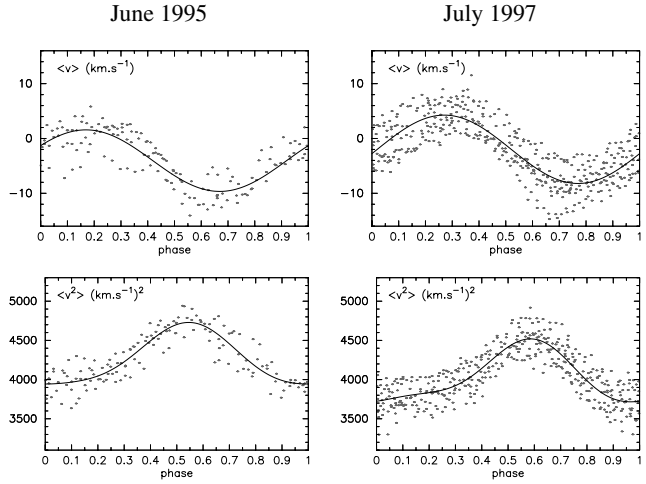

Fig. 5. $\langle v \rangle$ and $\langle v^2 \rangle$ calculated from the 4552.674 Å profiles of June 1995 and July 1997 fitted and folded with $f_1 = 4.679410$ c d^{-1} (*top*) and fitted with f_1 and $2f_1$ (*bottom*). The dots are the observations while the full line is the least-squares fit. The amplitudes of the variations in $\langle v \rangle$ and $\langle v^2 \rangle$ calculated from the dataset of June 1995 are significantly different from the corresponding amplitudes calculated from the dataset of July 1997, as shown in Table 1.

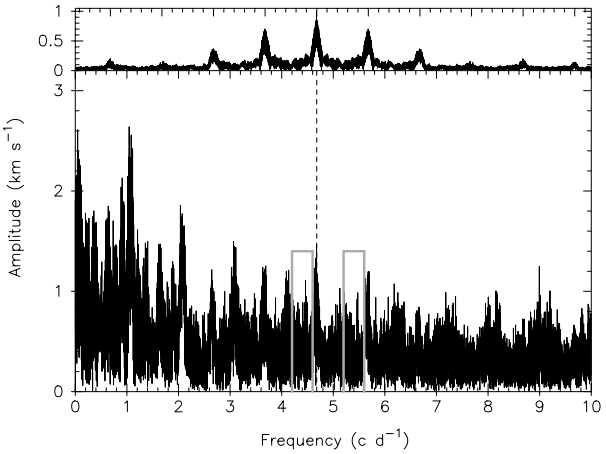

Fig. 6. Lomb-Scargle periodogram for $\langle v \rangle$ calculated from the 4552.654 Å profile after prewhitening with all frequencies listed in Table 3. The dashed line is drawn at the position of $f_1 = 4.679410$ c d^{-1} and shows that frequencies very close to f_1 are still present in the residuals of $\langle v \rangle$. The gray boxes mark the frequency regions that were used to determine the noise level.

The half width at half maximum of the amplitude of the highest peak of the window function associated to this subset turns out to be 0.077 c d^{-1}.

3.3.1. Frequency analysis for scalar quantities

The first three velocity moments calculated from the 421 spectra after prewhitening with f_1 and $2f_1$ showed again many peaks at the interval 0–2 c d^{-1}. In general, the shape of the window function was easily recognizable in the peak structures. Power was found at 0.09 c d^{-1}; 1.09 c d^{-1}; 2.09 c d^{-1}; etc. and 0.91 c d^{-1}; 1.91 c d^{-1}; etc. Because of aliasing it was very difficult to separate a frequency from its one-day alias. Although the interpretation of these frequencies is unclear, we prewhitened with them to search for other candidates in the 0–20 c d^{-1} interval. Except for a strong peak at 0.38 c d^{-1} and 0.44 c d^{-1}, or a frequency close to these values within the frequency resolution of 0.077 c d^{-1}, the highest amplitudes were reached for frequencies in the interval 3–6 c d^{-1}. Almost all peaks in this interval can be related, by means of peaks of the window function, to the following two frequencies: 3.89 c d^{-1} ($\langle v \rangle$ and $\langle v^3 \rangle$) and 5.37 c d^{-1} ($\langle v^2 \rangle$). Indications for this last frequency were also found in $\langle v \rangle$ and $\langle v^3 \rangle$ but with an amplitude lower than 4 *S/N*. In this subset of 8 nights we defined the *S/N* value as the average of the 50 highest peaks in the interval [2,8] c d^{-1}, which we scanned with frequency step 10^{-3} c d^{-1}, after prewhitening with the candidate frequencies listed in Table 3. An overview of the frequencies found in the three moments of the two bluest Si III lines of λ Scorpii is given in Table 2. All listed frequencies meet the requirements of the 4 *S/N* criterion applied to the subset of July 1997.

3.3.2. Frequency analysis across the profiles

Besides a one-dimensional frequency-analysis we also performed a two-dimensional analysis as described by Gies & Kullavanijaya (1988). This two-dimensional analysis (Intensity Period Search, IPS, Telting & Schrijvers 1997) is based on a CLEAN analysis (Roberts et al. 1987) of the variable signal in individual wavelength bins ($\Delta\lambda = 0.02$ Å) of a line profile. For each wavelength bin, the power of the frequencies is displayed as a grayscale value. We investigated the contribution of frequencies in the interval $[0, 20]$ c d^{-1}, with a frequency step of 0.001 c d^{-1}, to the variability of the Si III line profile at 4552.654 Å. We performed 400 iterations with a gain factor of 0.2. The periodogram is displayed in the left-hand panel of Fig. 7. Most power is found at f_1 and its aliases and harmonic frequencies.

After prewhitening with f_1 and its aliases and harmonics, the following frequencies showed up: 0.23 c d^{-1} and 1.09 c d^{-1} in the Si III 4542.654 Å profile and 0.13 c d^{-1} and 0.37 c d^{-1} in the Si III 4567.872 Å profile. We also found peaks at 9.72 c d^{-1} and 5.35 c d^{-1}. The latter frequency is located slightly below the 4 *S/N* level. We defined the *S/N* level of the IPS periodogram as the average of the power of the 50 highest peaks in the interval [2, 8] c d^{-1} after prewhitening with the frequencies mentioned in Table 2. The 4 *S/N* level is indicated as a horizontal gray line in the right-hand panel of Fig. 7.

3.4. The significant frequencies

The IPS analysis across the line profiles for the subset of July 1997 indicated the presence of at least two additional frequencies, 5.37 c d^{-1} and 3.89 c d^{-1}, which satisfy the 4 *S/N* criterion. These two frequencies agree within the accuracy with the frequencies $f_2 = 3.899013$ c d^{-1} and $f_3 = 5.340978$ c d^{-1} found in the periodogram of the whole dataset, as pointed out in Sect. 3.1. This suggests that f_2 and f_3 are real.

The candidate frequency 9.73 c d^{-1} only shows up in the IPS analysis of the 421 spectra of July 1997 and meets the 4 *S/N*

Table 2. An overview of all frequencies found in $\langle v \rangle$, $\langle v^2 \rangle$, and $\langle v^3 \rangle$ and from an IPS analysis of the Si III 4552.654 Å and 4567.872 Å profiles of the subset of July 1997, after prewhitening with f_1. The frequencies are ordered according to decreasing amplitude. For each frequency we list the amplitude (expressed in km s^{-1}, (km s^{-1})^2 or (km s^{-1})^3) between brackets. Frequencies that appear only in the analysis of the Si III 4552.654 Å respectively 4567.872 Å profile are marked with (^{a}) respectively (^{b}). All frequencies are given in c d^{-1} and satisfy the 4 *S/N* criterion.

421 spectra July 1997			
$\langle v \rangle$	$\langle v^2 \rangle$	$\langle v^3 \rangle$	IPS
0.09 (3.6)	0.11 (208)	1.09 (29957)	0.23(^{a}) (3.35)
0.38 (2.1)	0.44 (159)	0.37 (24852)	0.09(^{a}) (2.71)
3.89 (1.4)	5.37 (139)	4.90 (14022)	0.13(^{b}) (2.08)
			0.37(^{b}) (1.67)
			9.72 (1.65)
4 *S/N* = 1.1	4 *S/N* = 82	4 *S/N* = 13858	4 *S/N* = 1.52

criterion. It has no contribution to the velocity moments. A possible explanation could be that it is connected with a pulsation mode with high degree $l \geq 4$. In Table 5 (see the following section) we indeed find indications for an l-value higher than 5. A search for a peak near 9.72 c d^{-1} in the whole dataset leads to a value $f_4 = 9.726644$ c d^{-1}. The three additional frequencies are indicated by dotted lines in the Lomb-Scargle periodograms, given in Fig. 4.

In the panels of Fig. 7, the power spectrum of the IPS analysis is shown after prewhitening with f_1, f_2, f_3 and f_4 and their first harmonic. The 4 *S/N* level is indicated, as well as the position of the 4 frequencies.

All the significant frequencies are listed in Table 3, together with their contribution to the variations of $\langle v \rangle$ and $\langle v^2 \rangle$ of the two bluest lines of the Si III triplet of the whole dataset. We compare the contribution of a monoperiodic model with $f_1 = 4.679410$ c d^{-1} to the line-profile variability of λ Scorpii with the contribution of the model with 4 frequencies. In the case of $\langle v^2 \rangle$ we also took sum- and difference frequencies into account for the fit, as long as they turned out to have significant amplitudes. The model with 4 frequencies adds 7% to the total variance reduction of $\langle v \rangle$, which corresponds to a relative increase of 16% compared to the monoperiodic model for the 4552.654 Å profile. The model with 4 frequencies and its beat frequencies explains 43% of the variability of $\langle v^2 \rangle$, which represents a relative increase of the variance reduction with 23% compared to the model with f_1 alone.

4. Mode identification

For modelling the pulsational behaviour of λ Scorpii we combined the Moment Method (Briquet & Aerts 2003) and the IPS (Intensity Period Search) Method (Telting & Schrijvers 1997). We restricted to the intensive dataset obtained during the 8 nights of 1997, which was specifically gathered for this purpose, and adopted the following strategy.

First, we focussed on the dominant frequency and tried to find the best fitting set of pulsational parameters associated with this frequency. This neglect of the low-amplitude modes at first instance is justified as their amplitude is much lower (see Table 3). We analysed the theoretically generated time series with the Moment Method and the IPS Method in order to compare with the observational results. We especially focussed on a good reproduction of the phase and amplitude diagrams in the IPS method, since the diagrams are strongly related to different properties of the pulsation mode (see Schrijvers et al. 1997). The phase diagram is representative for the degree l, while the amplitude diagram contains additional information on other pulsational and stellar parameters. We studied the effect of small changes of the different free parameters on the shape of the diagrams. Through an iterative process between Moment Method and IPS Method we narrowed the acceptable interval of best fitting parameters.

Secondly, we used the best fitting stellar parameters obtained from the modelling of the first frequency in an attempt to associate pulsational parameters to the lower-amplitude frequencies.

4.1. The moment method

The latest version of the Moment Method (Briquet & Aerts 2003) was used to identify the main mode of λ Scorpii. We did not attempt identifying the other, low-amplitude modes with this method, as the relative accuracy of their amplitudes in $\langle v^2 \rangle$ and $\langle v^3 \rangle$ is rather low. To remove the contribution of the low-amplitude frequencies for the mode identification of the main mode, we averaged all 421 observed profiles in phase bins of 0.025 of the main oscillation cycle before re-calculation of the moment values.

We calculated the discriminant γ_l^m for the following ranges of free parameters: $i \in [0, 90]$, $v_{\rm p} \in [4, 22]$, $v \sin i \in [60, 250]$, $\sigma \in [5, 30]$, $l \in [1, 6]$, $-l \leq m \leq l$ (we refer to Briquet & Aerts 2003 for a meaning of the symbols). The amplitude of the first moment calculated from the 4552.654 Å respectively 4567.872 Å profile of the 40 averaged spectra was respectively 5.8 km s^{-1} and 6.0 km s^{-1} for f_1, which is a slight increase compared to the values listed in Table 3. The Moment Method resulted in a preference for an $(1, -1)$ or $(2, -1)$ mode associated with f_1. An overview of the lowest values γ_l^m (corresponding to the most likely mode identifications) is listed in Table 4. The analysis of the two bluest Si III lines led to consistent results. We note that the values of γ_l^m are relatively high in comparison with the ones obtained for other stars (e.g. Briquet & Aerts 2003). This is probably due to the averaging proces for the additional low-amplitude modes. The discriminant is unable to distinguish between the $(1, -1)$ and $(2, -1)$ mode. We also point out that the continuous free parameters i and $v \sin i$ cannot be derived accurately with this method, as discussed by De Ridder et al. (2005).

4.2. The intensity period search (IPS) method

In a first step we calculated the IPS diagnostic diagrams for the 4 frequencies listed in Table 3 and their first harmonic to estimate their value of l and $|m|$. Prograde and retrograde modes can be distinguished my means of a blue-to-red respectively

Table 3. Contribution of a monoperiodic model and a model with 4 frequencies to the variations of $\langle v \rangle$ and $\langle v^2 \rangle$ of the Si III 4552.654 Å and 4567.872 Å profiles for the whole dataset. For every frequency, the corresponding amplitude (expressed in km s^{-1} respectively (km s^{-1})^2) with its standard error (s. e.) is given. In the case of $\langle v^2 \rangle$ the contribution, if significant, of the expected beat frequencies are taken into account. The frequencies are given in c d^{-1}. Note that 9.72c d^{-1} has no contribution in the velocity moments. The total variance reduction (frac. var.) of each model is also given.

$$f_1 = 4.679410 \text{ c d}^{-1}$$
$$f_2 = 3.899013 \text{ c d}^{-1}$$
$$f_3 = 5.340978 \text{ c d}^{-1}$$
$$f_4 = 9.726644 \text{ c d}^{-1}$$

$\langle v \rangle$					
Si III 4552.654 Å			Si III 4567.872 Å		
Freq.	Ampl. ± s. e.	Frac. var.	Freq.	Ampl. ± s. e.	Frac. var.
f_1	5.27 ± 0.22	43.98%	f_1	5.34 ± 0.26	36.03%
f_1	5.28 ± 0.21		f_1	5.34 ± 0.25	
f_2	1.94 ± 0.21		f_2	2.25 ± 0.25	
f_3	0.70 ± 0.21		f_3	0.63 ± 0.25	
f_4	–	50.89%	f_4	–	42.96%

$\langle v^2 \rangle$					
Si III 4552.654 Å			Si III 4567.872 Å		
Freq.	Ampl. ± s. e.	Frac. var.	Freq.	Ampl. ± s. e.	Frac. var.
f_1	340 ± 18		f_1	341 ± 19	
$2f_1$	71 ± 18	35.27%	$2f_1$	74 ± 19	30.59%
f_1	326 ± 17		f_1	329 ± 18	
$2f_1$	76 ± 17		$2f_1$	76 ± 18	
f_2	48 ± 17		f_2	78 ± 18	
f_3	133 ± 17		f_3	136 ± 18	
f_4	–		f_4	–	
$f_1 - f_2$	99 ± 17		$f_1 - f_2$	109 ± 20	
$f_1 + f_2$	35 ± 17		$f_1 - f_3$	86 ± 20	
$f_2 - f_3$	36 ± 17	43.33%	$f_2 - f_3$	71 ± 18	41.86%

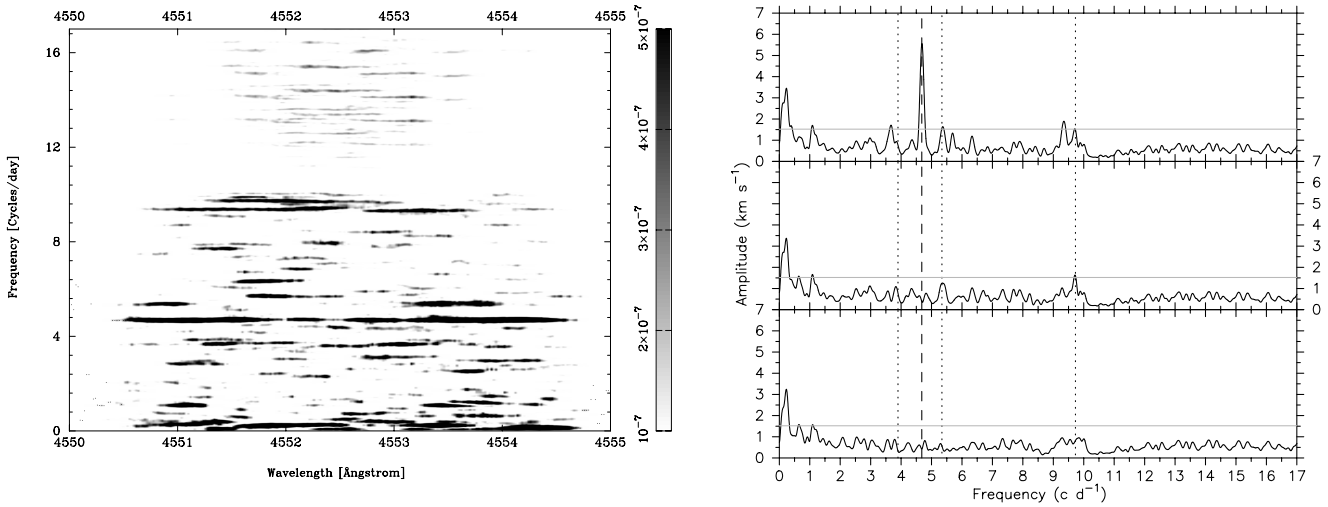

Fig. 7. Power spectrum (*left*) and summed periodogram across the line profile (*right*) of the Si III line at 4552.654 Å of λ Scorpii, obtained by an IPS analysis. For each wavelength bin the power as a function of frequency is coded in gray. *Left*: power spectrum of the data. The main peak occurs at the frequency f_1. *Right*: summed periodograms of the original data, of the data after prewhitening with f_1 and its first harmonic and of the data after prewhitening with all the frequencies listed in Table 3 and their first harmonic. The horizontal light gray line shows the 4 *S/N* level. f_1 is indicated by a dashed line while the positions of f_2, f_3 and f_4 are marked by a dotted line.

Table 4. The results of the Moment Method for the main mode of λ Scorpii. The lowest minima of the discriminant γ_l^m for f_1 are listed. $v \sin i$ is given in km s^{-1}; i in °.

Si III 4552.654 Å					Si III 4567.872 Å				
l	m	γ_l^m	$v \sin i$	i	l	m	γ_l^m	$v \sin i$	i
1	–1	9.8	128	45	1	–1	9.8	118	40
2	–1	9.9	120	50	2	–1	9.9	118	50
3	–1	12.3	120	89	2	–2	12.5	118	90
2	–2	13.2	118	89	3	–1	13.0	116	85
1	0	16.4	122	75	1	0	16.9	122	80

red-to-blue descent of the phase through the profile. However, in special cases of fast rotation or high $|m|$-values a retrograde mode in the corotating frame can be confused with a prograde mode in the observer's frame.

We used different methods to calculate the diagrams: the IPS periodogram, a single-sinusoid fit and a double-sinusoid fit. Figure 8 shows the mean profile of the observed data (top), the phase distribution (middle) and amplitude distribution (bottom) across the line profile for each of the 4 frequencies. All frequencies lead to well-defined phase curves, which illustrates that these frequencies are indeed present in the data. The phase curves of the first harmonics are much noisier. We note that the amplitude- and phase diagrams associated with a double-sinusoid fit with f_i and $2f_i$ are similar to the ones obtained from a single-sinusoid fit with f_i. The amplitudes obtained from an IPS analysis are in general lower than the ones obtained from a single-sinusoid fit. This is caused by the subtraction of a small amount of the power, depending on the gain value of the IPS analysis.

Telting & Schrijvers (1997) derived the following relationships between l and phase difference $\Delta\Psi_{f_1}$, respectively $|m|$ and $\Delta\Psi_{2f_1}$:

$$l \approx 0.10 + 1.09|\Delta\Psi_{f_1}|/\pi, \quad (1)$$

$$|m| \approx -1.33 + 0.54|\Delta\Psi_{2f_1}|/\pi. \quad (2)$$

For the first frequency f_1 (top left panel of Fig. 8) we can read off a blue-to-red phase difference $\Delta\Psi_{f_1}$ of 1.5π radians, implying $l = 1.5 \pm 1$; the phase diagram of $2f_1$ shows a phase difference of 4π radians, hence $|m| = 2 \pm 2$. These (l, m)-values are compatible with the best results derived from the Moment Method (Table 4).

The results for the additional frequencies are sumarized in Table 5. These first estimates of l and $|m|$ need further investigation through detailed modelling of the line diagnostics.

4.3. Modelling of the IPS diagnostics

In a next step we generated theoretically calculated time series by means of a FORTRAN code which took both temperature changes (dT/T) and EW changes due to dT/T into account (Schrijvers & Telting 1999) for the main frequency. Subsequently we compared the IPS diagnostics obtained from the generated data with those of the observed data in order to find the set of parameters which lead to the best reconstruction of the observed phase and amplitude diagrams. We used the same 421 HJDs as occur for the observed time series. We calculated time series with different values of the following free stellar parameters: inclination i, $v \sin i$, intrinsic line width σ, linear limb-darkening coefficient α and EW response to temperature changes. The free mode parameters are the degree l, the azimuthal number m, the amplitude of the pulsation $v_{\max}$, the ratio of horizontal to vertical pulsation amplitude k and the ratio of rotational, pulsational frequency Ω/ω, and amplitude of temperature variations dT/T.

Table 5. Blue-to-red phase differences of f and its first harmonic, together with estimates for l and m according to Eqs. (1) and (2) for the 4 frequencies listed in Table 3 obtained from the IPS method. The phase differences $\Delta\Psi$ are given in π radians; the frequencies are expressed in c d^{-1}. Whenever the 4552.654 Å (^{a}) and 4567.872 Å (^{b}) profiles gave different phase differences we listed the two values.

Frequency	$\Delta\Psi_f$	$\Delta\Psi_{2f}$	l	$\lvert m\rvert$	
f_1 4.679410	1.5	4	1.5 ± 1	2 ± 2	($^{a+b}$)
f_2 3.899013	2.5	4	2.5 ± 1	2 ± 2	($^{a+b}$)
f_3 5.340978	2.5	6	2.5 ± 1	3 ± 2	(^{a})
	2.5	7	2.5 ± 1	3.5 ± 2	(^{b})
f_4 9.726644	6.5	≤ 6	6.5 ± 1	≤ 3	(^{a})
	6.5	7.5	6.5 ± 1	3.5 ± 2	(^{b})

In first instance we only took the pulsation mode for f_1 into account. Since the theoretical models are based on many free parameters it was a time consuming task to find the best fitting parameters. We note that we took full account of the relations between Ω/ω, k and $v \sin i$ while calculating the different grids of parameters, in order to constrain to physically relevant cases.

As different combinations of different parameters lead to similar reproductions of the line profile, we were only able to define intervals of best-fitting parameters. An iterative process resulted in the following set of stellar parameters: $70° \leq i \leq 90°$; $v \sin i \sim 125$ km s^{-1}, intrinsic line width $\sigma \sim 18.75$ km s^{-1}, $\alpha \sim 0.3$, $0.63 \leq EW$ response ≤ 0.83. The obtained range for the inclination angle is fully compatible with the one derived for the orbital inclination of the close orbit in Paper I. For stars with effective temperatures near 25 000 K we expect α to be clearly below 1, on theoretica grounds, while this value is predicted to be above 1 for stars with effective temperatures near 22 000 K (De Ridder 2001). This is an additional argument that the variability with f_1 is due to the primary.

In Fig. 9 we confront the observed mean profile and IPS diagnostics of f_1 with the theoretical ones, based on models with combinations of l and m as suggested by the IPS Method. Both $(1, -1)$ and $(2, -1)$ represent the observed phase diagram well. However, the amplitude diagram of $(1, -1)$ gives a better approximation of the two-peaked observed amplitude diagram associated with f_1 and represents in a better way the shape of the amplitude diagram associated with $2f_1$ than $(2, -1)$. We therefore prefer $(1, -1)$, with the following best fitting pulsational parameters: $(1, -1)$, $v_{\max} \sim 14$ km s^{-1}, $k \sim 0.20$, $\Omega/\omega \sim 0.098$, and $0.02 \leq \mathrm{d}T/T \leq 0.04$. We note that we found indications for a relative high k-value of approximately 0.20. This high value

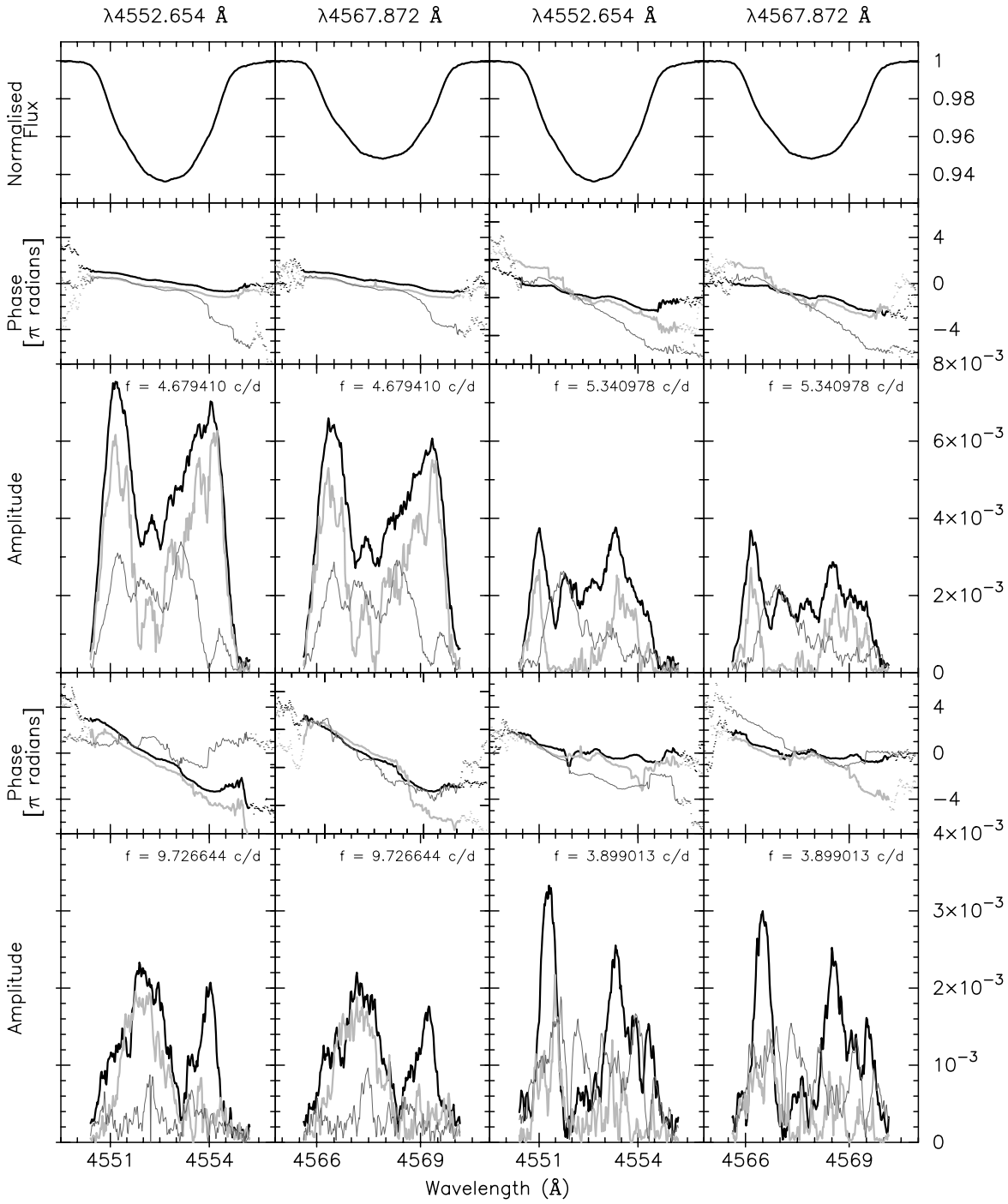

Fig. 8. Mean profile and IPS diagrams for the variability in the 4552.654 Å and 4567.872 Å line profile at f_i and its first harmonic, with f_i indicated in the panels: f_1 (*top panels, left*); f_3 (*top panels, right*), f_4 (*bottom panels, left*), and f_2 (*bottom panels, right*). The phase diagrams (*middle of each panel*) are expressed in π radians. The amplitude diagrams (*bottom of each panel*) give the amplitude of the variations of respectively f_i and $2f_i$ in the line profiles expressed in units of normalised flux. Thick black line: single-sinusoid fit f_i; light gray line: CLEANed Fourier transform f_i; thin black line: single-sinusoid fit $2f_i$. Note the difference in scale of the amplitude diagrams in the upper and lower panels.

was needed to explain the concentration of the variability of amplitude in the wings of the profile (two-peaked structure) associated with f_1 (see Fig. 8). As pointed out by Schrijvers et al. (1997) this particular shape can be represented by relative high k-values.

An attempt to extend the models of the theoretical profiles to more than one pulsation mode turned out to be difficult. Adding more modes to the model implied adding several free parameters. Since the mode parameters of the different modes were mutually linked, the IPS diagnostics changed drastically with every change of a parameter for the low-amplitude modes. Therefore, it was not possible to come to a best set of mode parameters for the additional frequencies. However, because of the dominant character of f_1, the diagnostics associated with f_1 were always stable for all calculated multiperiodic models.

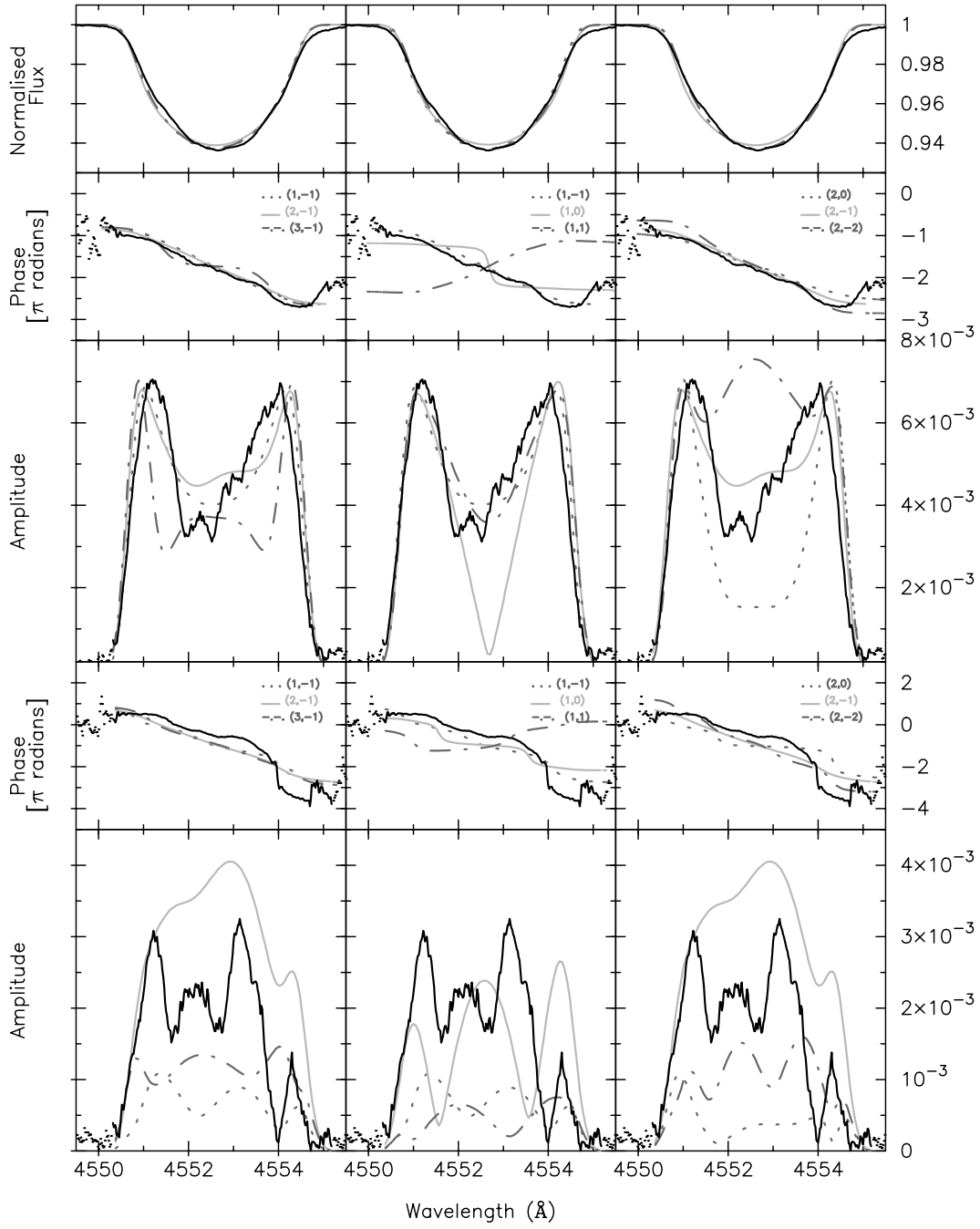

Fig. 9. Mean profile, phase and amplitude diagrams of frequency f_1 (*top*) and $2f_1$ (*bottom*) in the wavelength region of the 4552.654 Å line, as calculated from single-sinusoid fits. The solid black line represents the diagnostics derived from the observed data. The other lines are derived from theoretically calculated profiles with parameters: $v \sin i = 125$ km s^{-1}, $i = 80°$, $\sigma = 18.75$ km s^{-1}, $\mathrm{d}T/T = 0.03$ and $k = 0.20$. *Left panel*: $m = -1$ and different values of l: $l = 1$ (dotted dark gray line), $l = 2$ (solid light gray line) or $l = 3$ (dashed-dotted dark gray line). *Middle panel*: $l = 1$ and different values of m: $m = -1$ (dotted dark gray line), $m = 0$ (solid light gray line) or $m = 1$ (dashed-dotted dark gray line). *Right panel*: $l = 2$ and different values of m: $m = 0$ (dotted dark gray line), $m = -2$ (solid light gray line) or $m = -2$ (dashed-dotted dark gray line). The phases are given in π radians; the amplitudes are expressed in terms of normalised flux of the line profile.

5. The possibility of resonant excitation

Due to the binary nature and the short orbital period of the close orbit of λ Scorpii, the question may be raised whether some of the observed modes are excited by the tidal action exerted by the companion. In order to investigate this possibility, we followed the procedure outlined by Willems & Aerts (2002) and determined the amplitude of the tidally induced radial-velocity variations for several appropriate stellar models as a function of the uncertain rotational angular frequency Ω. It follows that for the orbital period of $5\overset{\mathrm{d}}{.}9525$ days, the orbital eccentricity $e = 0.26$, and the admissible range of rotational angular velocities Ω resulting from the projected rotational velocity $v \sin i \sim 125$ km s^{-1} and $70° \leq i \leq 90°$, resonant excitation of high-order g^+-modes can yield radial-velocity

variations with amplitudes of several km s^{-1}. However none of the eigenfrequencies of the observed oscillation modes listed in Table 5 is close to an integer multiple of the orbital frequency $f_{\rm orb} = 0.167996$ c d^{-1}, which is essential for resonant excitation or enhancement to occur. In addition, even if some of the eigenfrequencies were close to an integer multiple of the orbital frequency, the involved harmonic of the tidal potential would be of such a high order (at least 20) that resonant excitation would be very unlikely. The observed frequencies therefore most likely belong to the intrinsic oscillation modes of the primary or tertiary star in λ Scorpii.

We point out that the frequency 0.09 c d^{-1} listed in Table 2 may be related to the orbital frequency, but the complicated window function makes it not possible to draw any conclusions on its role.

6. Conclusions

We subjected the line-profile variations in the Si III lines at 4552.7 Å, 4567.9 Å of a time series of the multiple stars λ Scorpii, spanning more than 5000 days, to a detailed analysis. We found indications for the variable character of the dominant frequency near $f_1 = 4.679410$ c d^{-1}. This result is entirely compatible with the one obtained by Lomb & Shobbrook (1975) and is easily explained in terms of the light-time effect in the multiple system. Due to the limits of the dataset, we were unfortunately unable to measure the rate of change of the frequency. We strongly suspect that f_1 is an oscillation mode associated to the primary of λ Scorpii. Given an overall broadening of 140 km s^{-1}, respectively 160 km s^{-1} for the primary, respectively tertiary (see Paper I), and the lower flux of the tertiary, we expect that the signature associated to possible oscillations of the tertiary will be smeared out and will have a non-detectable contribution to the combined profiles. The reasonably good modelling of the average profile by means of an oscillation with f_1 as shown in Fig. 9, supports this suspicion.

The unability to remove the contribution of the variable frequency f_1 hampered the search for, and an accurate determination of additional frequencies in the full dataset. The analysis of a subset, comprising the 8 nights of intensive monitoring, allowed the confirmation of three additional significant frequencies: $f_2 = 3.899013$ c d^{-1}, $f_3 = 5.340978$ c d^{-1} and $f_4 = 9.726644$ c d^{-1}. All of them are explained in terms of nonradial pulsation modes.

We were able to associate a (1, –1) mode to the dominant frequency and to put constraints on the values of the velocity parameters of λ Scorpii, among which $70^\circ \leq i \leq 90^\circ$ and $v \sin i \sim 125$ km s^{-1}. As the additional frequencies had much lower amplitudes than the one of the dominant frequency, we were unable to unravel a fully unique multiperiodic model.

It is unlikely that the modes of λ Scorpii are enhanced or excited by means of tidal forcing. λ Scorpii is one case study in our observational project to search for tidal effects on pulsation modes in nonradially pulsating B-type stars in close binaries. A few examples of tidal forcing on NRP are suggested for β Cephei stars in the literature, e.g. σ Scorpii ($P_{\rm orb} = 33^{\rm d}$, $e = 0.40$, Fitch 1967), α Virginis ($P_{\rm orb} = 4^{\rm d}$, $e = 0.15$, Smith 1985a,b), η Orionis ($P_{\rm orb} = 8^{\rm d}$, $e = 0.011$, De Mey et al. 1996). We will continue the search for resonant excitation due to binarity by means of a systematic observational study of some more selected early B-type pulsators in close binaries in order to understand better the conditions needed for tidally induced oscillations. A first qualitative step to a theoretical investigation on the conditions favourable for the resonant excitation of free oscillation modes can be found in Willems (2003).

Acknowledgements. The authors would like to thank A. Claret for providing a set of theoretical stellar models. BW acknowledges the support of the British Particle Physics and Astronomy Research Council (PPARC) and of NASA ATP grant NAG5-13236 to Vicky Kalogera. KU is supported by the Fund of Scientific Research - Flanders (FWO), under project G.0178.02.

References

Aerts, C., De Pauw, M., & Waelkens, C. 1992, A&A, 266, 294
Aerts, C. 1996, A&A, 314, 115
Aerts, C., De Cat, P., Cuypers, J., et al. 1998, A&A, 329, 137
Balona, L. 1986, MNRAS, 219, 111
Berghöfer, T. W., Schmitt, J. H. M. M., & Cassinelli, J. P. 1996, A&AS, 118, 481
Breger, M. 1993, in Stellar Photometry – Current Techniques and Future Developments, ed. C. S. Butler, & I. Elliott (Cambridge Univ. Press), IAU Coll., 136, 106
Brown, A. G. A., & Verschueren, W. 1997, A&A, 319, 811
Buscombe, W. 1969, MNRAS, 144, 31
Briquet, M., & Aerts, C. 2003, A&A, 398, 687
Cuypers, J. 1987, The Period Analysis of Variable Stars, Academiae Analecta, Royal Academy of Sciences, 49(3) (Belgium)
De Mey, K., Aerts, C., Waelkens, C., & Van Winckel, H. 1996, A&A, 310, 164
De Mey, K. 1997, Ph.D. Thesis, Katholieke Universiteit Leuven, Belgium
De Mey, K., Aerts, C., Waelkens, C., et al. 1997, A&A, 324, 1096
De Ridder, J. 2001, Ph.D. Thesis, KULeuven
De Ridder, J., Molenberghs, G., & Aerts, C. 2005, Appl. Stat., 54, 1
Fitch, W. S. 1967, ApJ, 148, 481
Giacconi, R., Branduardi, G., Briel, U., et al. 1979, ApJ, 230, 540
Gies, D. R., & Kullavanijaya, A. 1988, ApJ, 326, 813
Gulati, R. K., Malagnini, M. L., & Morossi, C. 1989, A&AS, 80, 73
Hadrava, P. 1995, A&AS, 114, 393
Handler, G., Shobbrook, R. R., Jerzykiewicz, M., et al. 2004, MNRAS, 347, 454
Harmanec, P., Uytterhoeven, K., & Aerts, C. 2004, A&A, 422, 1013
Heynderickx, D., Waelkens, C., & Smeyers, P. 1994, A&AS, 105, 447
Hoffleit, D. 1982, The Bright Star Catalogue, Yale University Observator, New Haven, Connecticut, USA
Lomb, N. R., & Shobbrook, R. R. 1975, MNRAS, 173, 709
Léhmann-Filhés, R. 1894, Astron. Nachr., 136, 17
Lesh, J. R., & Aizenman, M. L. 1978, ARA&A, 16, 215
Pasinetti Fracassini, L. E., Pastori, L., Covino, S., & Pozzi, A. 2001, A&A, 367, 521
Pamyatnykh, A. A. 1999, AcA, 49, 119
Roberts, D. H., Lehar, J., & Dreher, J. W. 1987, AJ, 93, 968
Sareyan, J. P., Chauville, J., Chapellier, E., & Alvarez, M. 1997, A&A, 321, 145

Scargle, J. D. 1982, ApJ, 263, 835
Schrijvers, C., Telting, J. H., Aerts, C., Ruymaekers, E., & Henrichs, H. F. 1997, A&AS, 121, 343
Schrijvers, C., & Telting, J. H. 1999, A&A, 342, 453
Shobbrook, R., & Lomb, N. R. 1972, MNRAS, 156, 181
Slipher, V. M. 1903, Lick. Obs. Bull., 1, 23
Smith, M. A. 1985a, ApJ, 297, 206
Smith, M. A. 1985b, ApJ, 297, 224
Stellingwerf, R. F. 1978, ApJ, 224, 953
Stoeckley, T. R., & Buscombe, W. 1987, MNRAS, 227, 801
Telting, J. H., & Schrijvers, C. 1997, A&A, 317, 723
Uytterhoeven, K., Briquet, M., Aerts, C., et al. 2004a, A&A, submitted
Uytterhoeven, K., Willems, B., Lefever, K., et al. 2004b, A&A, 427, 581 (Paper I)
Vogt, S. S., & Penrod, G. D. 1983, ApJ, 275, 661
Watson, R. D. 1971, Ph.D. Thesis, Mount Stromlo Observatory
Watson, R. D. 1988, Ap&SS, 140, 255
Westin, T. N. G. 1985, A&AS, 60, 99
Willems, B., & Aerts, C. 2002, A&A, 384, 441
Willems, B. 2003, MNRAS, 346, 968